A 200Gb/s QAM-16 Silicon Photonic Transmitter with 4 Binary-Driven EAMs in An MZI Structure

Arian Hashemi Talkhooncheh[1], Aaron Zilkie[2], Guomin Yu[2], Roshanak Shafiiha[2], Azita Emami[1]
[1] California Institute of Technology, 1200 E California Boulevard, Pasadena, California, USA, ahashemi@caltech.edu
[2] Rockley Photonics Inc., Pasadena, CA, USA, aaron.zilkie@rockleyphotonics.com

Abstract: A DAC-less 200Gb/s QAM-16 transmitter in a multi-micron silicon-photonics platform using 4 binary-driven SiGe EAMs in an unbalanced MZI is presented. The transmitter exhibits bit-error rates of 3×10^{-4} and 2.8×10^{-4} for square and hexagonal constellations.

1. Introduction

Highly-integrated optical interconnects in silicon photonics are growing as preeminent platforms for the next generation optical transceivers for inter- and intra-datacenter applications. Multi-point Quadrature-Amplitude Modulation (QAM-N) is a promising modulation scheme that increases the overall bandwidth density efficiency in coherent applications. However, the inherent optical power penalty imposes demanding linearity requirements on analog link components, which results in power hungry electronics. Generating QAM-16 constellations can be achieved using several optical and electrical circuit architectures. One common way of generating a square QAM-16 constellation is through two 4-level amplitude modulators nested in an in-phase/quadrature (I/Q) modulator. Each 4-level amplitude modulator could be implemented by either a single optical modulator and a 4-level driving signal, or 2 phase/amplitude modulators, placed in parallel, and driven by on-off-keying (OOK) signals [1, 2, 3]. Hexagonal QAM-16 constellations benefit from triangular latices, which result in 10% reduction in required power to generate a square QAM-16 constellation of the same lattice size. Hexagonal QAM-16 constellations, unlike square QAM-16, are only realizable via 4 parallel amplitude modulators.

The choice of the optical modulator for the design of a QAM-16 transmitter directly affects the overall transmitter performance metrics, such as the overall constellation size, bit-error-rate (BER), and electro-optical power penalties. Travelling-wave and lumped phase modulators require relatively large voltages (large $V_{\pi}L$) and power-hungry electrical drivers while having lower bandwidth due to excessive microwave losses and large capacitive parasitics [4]. Moreover, these phase modulators should exhibit π phase shift at high speeds to maximize the size of the QAM-16 constellation, since lower phase shift angles will result in a shrunk and rotated constellation. Despite their compact dimensions, silicon photonic ring modulators require careful temperature stabilization, while their undesired phase modulation (modulation chirp) should be compensated when placed in parallel [5]. Electro-absorption modulators (EAMs) do not suffer from the mentioned limits due to their smaller footprints and lower voltage requirements, which make them attractive for high-speed modulation and dense integration with low pJ/bit energy efficiencies [6, 7, 8, 9]. However, their performance for QAM-N is limited by non-linearities in the optical transfer function, maximum input optical power, and modulation chirp. In this work we show an optical signal-to-noise ratio (OSNR)-optimized design of a DAC-less 200 Gb/s QAM-16 transmitter using 4 binary-driven SiGe EAMs placed in an unbalanced 5-arm MZI structure, and experimentally demonstrate square and hexagonal QAM-16 generation with optimal power penalties and BER performance.

2. QAM-16 Transmitter Design

The proposed photonics circuit architecture of the QAM-16 transmitter is shown in Fig. 1(a). The circuit includes 4 identical EAMs in an unbalanced 5-arm interferometer. All EAMs have same lengths, so that they exhibit equal modulation chirp, when driven with same driving voltage levels. This will ensure constellation symmetry for both square and hexagonal formats. The optional 5th interferometric arm is incorporated in the design to move the generated off-centered constellation back to the origin and avoid sending extra optical power into the link. This arm could alternatively be used to adjust the optical power of the carrier signal sent into the link.

All design parameters such as EAM lengths, optical power levels entering each arm, driving voltage amplitude, and the relative static optical phase difference between arms are included in the optimization problem, shown in Fig. 1(b). The 5×1 coupler is considered to have power combining ratios k_1 through k_5 that need to be optimized based on EAM characteristics and to minimize the required total optical input power. The EAM placed on the *i*-th arm receives the optical power $P_{in,\, i}$ (with an optical vector field $E_{in,\, i}$). The output optical field of each EAM is denoted by $E_{EAM,\, i}$, which is equal to $E_{in,\, i}\times L$ for the ON state, or $E_{in,\, i}\times L\times R\times e^{j\varphi(V)}$ for the OFF state, in which L stands for the EAM insertion loss (IL), R stands for the EAM extinction ratio (ER), and $\varphi(V)$ denotes the EAM modulation chirp in

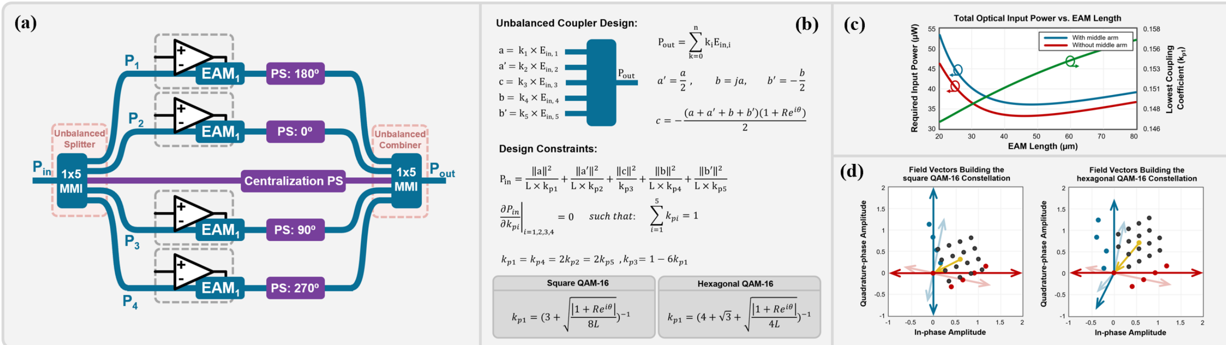

Figure 1: (a) System block diagram of the optical QAM-16 transmitter. (b) Proposed optimization problem to solve for unbalanced 1×5 splitting/coupling ratios. (c) EAM length optimization. (d) Optimized field vectors constructing the QAM-16 constellation.

radians, when driven by a signal of amplitude V. As shown at the bottom of Fig. 1(b), the required coupling coefficients of the 5×1 combiner is calculated for both QAM-16 formats. The EAM lengths should still be optimized separately. Increasing the EAM lengths would provide more ER, however, the IL and the modulation chirp also increase. The plot shown in Fig. 1(c) shows the required optical input power, with/without the centralization arm power included. This plot is generated for the Si-Ge FK-EAMs used in this design, resulting in optimized EAM lengths of 78 µm. The plots in Fig. 1(d) depict the resulting square and hexagonal QAM-16 constellations, along with the 4 pairs of field vectors representing the ON/OFF states of each modulating arm.

The power splitting/combining ratios of the 1×5 couplers are derived as 1:2:0.78:2:1. The structure shown in Fig. 2(a) is proposed to generate the uneven splitting/combining ratios. The benefits of this structure compared to cascaded 1×2 couplers and star couplers are superior robustness across temperature, wavelength, and process variations, in addition to lower overall insertion loss. As shown in Fig. 2(a), A balanced 1×7 MMI is put at the input to split the incoming power into 7 equally-split outputs. Outputs 2, 3, 5 and 6 are phase matched via waveguide tapering, and are fed to balanced 2×1 MMIs to constructively combine their optical power. In order to achieve the desired splitting factor for the middle arm, an unbalanced 1×2 MMI is designed to keep 78% of the optical power and dissipate the rest. This is achieved by introducing an asymmetricity to a balanced 1×2 MMI, as shown in Fig. 2(b). Starting from a balanced MMI, a rectangular piece with a length lower than the total length of the MMI region is removed. This cut piece directs the power concentration of the MMI optical modes into one output. While the photonics circuit can be redesigned for the hexagonal format, we experimentally show that the design optimized for the square format can also be used for the hexagonal version, since the only difference in the hexagonal setting is the power splitting ratios and the relative static phase differences between the arms.

3. Experimental Results

The photonic integrated circuit proposed in section II was fabricated in Rockley Photonics multi-micron Si-photonics platform, which is an EAM-based high-speed platform optimized for high density integration, low power consumption, and co-packaged optics [6, 7]. Fig. 2(c) shows the optical measurements of the custom-designed 1×5 splitter/coupler. The laser input power was set at 0-dBm, and the 5 optical output levels were measured across wavelengths from 1500nm to 1630nm and temperatures from 30ºC to 60ºC. Maximum output power imbalance at each wavelength was measured at 0.21dB. The overall IL of the structure at the operating point of 55ºC and 1550nm was measured at 0.44dB, with fiber-to-chip edge coupling losses of approximately 6.4dB.

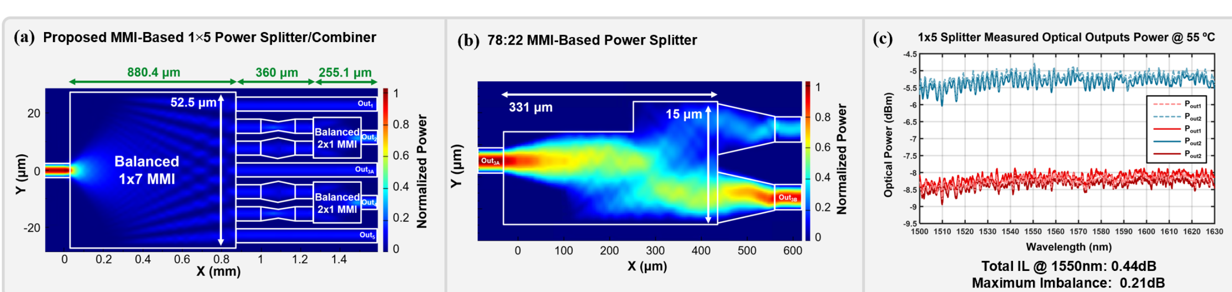

Figure 2: (a, b) Proposed MMI-base unbalance 1×5 power splitter/combiner. (c) Measured optical output levels of the proposed coupler.

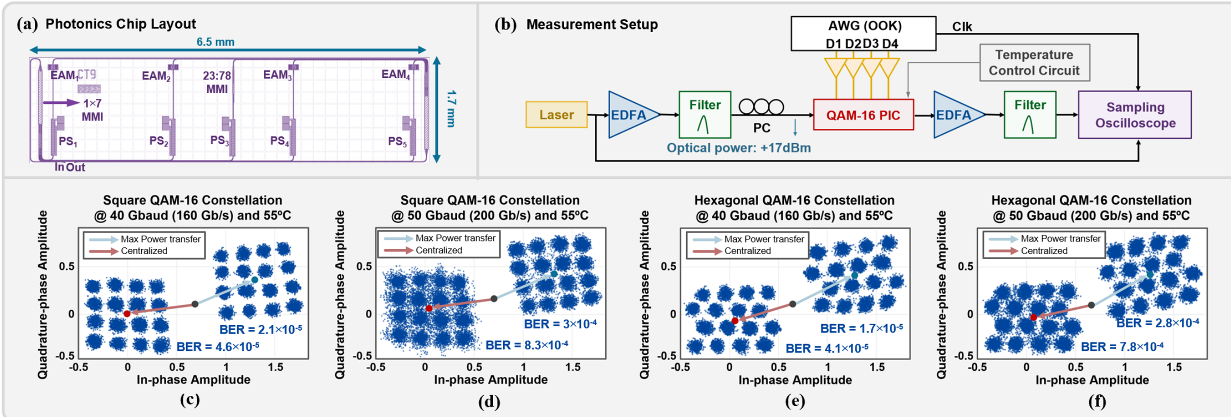

Figure 3: (a) Fabricated photonics chip layout. (b) Measurement setup. (c-f) Measured square and hexagonal QAM-16 constellations.

The complete layout of the proposed QAM-16 optical transmitter is shown in Fig. 3(a). The static optical phase shifts between arms are generated by applying DC voltages to thermal phase shifters on each arm. The measurement setup is shown in Fig. 3(b). The optical signal is amplified prior to the chip to improve the OSNR. An arbitrary waveform generator provides 40 to 50 Gb/s PRBS-31 data streams for 4 high-speed probes, which drive all EAMs with $2V_{PP}$ amplitudes. The transmitter output is monitored using a high-speed coherent sampling oscilloscope, with an internal 90-degree hybrid and a self-homodyne detection architecture. Fig. 3(c, d) show measured square QAM-16 constellations at 40 Gbaud (160 Gb/s) and 50 Gbaud (200 Gb/s), respectively. Each figure shows measurements under two settings, when the middle arm is used to centralize the constellation, or to shift it away from the origin. As shown in both figures, the middle arm can successfully centralize the constellation. Depending on the receiver and the detection architecture, the off-centered versions with extra average power can be fed into the link.

For the hexagonal format, the optical power ratio into the 4^{th} arm should be reduced to 1.73, and the relative phase shift of the 5^{th} arm should be changed to 240º. These changes were implemented on the existing chip, which was optimized for the square format, using the thermal phase shifters and the driving voltage levels for arms 4 and 5. Fig. 3(e, f) show the measurements results for the hexagonal format at 40 Gbaud and 50 Gbaud, respectively. For all measurements shown in Fig. 3(c-f), the BER were measured at an OSNR of 35dB. As shown in the figures, the hexagonal settings show superior BER performance compared to their corresponding square versions.

4. Conclusion

In this work, a silicon photonic QAM-16 transmitter with 4 SiGe EAMs in parallel within an unbalanced MZI structure is demonstrated. The fabricated chip performs QAM-16 transmission at 200 Gb/s with 3×10^{-4} and 2.8×10^{4} of BER at an OSNR level of 35 dB for square and hexagonal constellations. This scheme can similarly be applied to design 200 Gb/s QAM-16 Si-photonic transmitters in the O-band using hybrid-integrated InP-based EAMs with < 1pJ/bit power consumption [6, 7] to provide a path to 400 Gb/s/λ transmitters.

5. References

[1] C. R. Doerr, L. Zhang, P. J. Winzer and A. H. Gnauck, "28-Gbaud InP square or hexagonal 16-QAM modulator," 2011 Optical Fiber Communication Conference and Exposition and the National Fiber Optic Engineers Conference, 2011, pp. 1-3.

[2] Shuangyi Yan, Xuan Weng, Yuliang Gao, Chao Lu, Alan Pak Tao Lau, Yu Ji, Lei Liu, and Xiaogeng Xu, "Generation of square or hexagonal 16-QAM signals using a dual-drive IQ modulator driven by binary signals," Opt. Express 20, 29023-29034 (2012)

[3] F. Fresi, J. Klamkin, A. Malacarne and L. Potì, "Versatile low-complex 16-QAM optical transmitter driven by binary signals," 2012 IEEE Globecom Workshops, 2012, pp. 336-339, doi: 10.1109/GLOCOMW.2012.6477593.

[4] A. Samani et al.,"Silicon photonic Mach–Zehnder modulator architectures for on chip PAM-4 signal generation," J. Lightwave Technol. 37,2989-2999(2019)

[5] Y. Tong et al., "An experimental demonstration of 160-Gbit/s PAM-4 using a silicon micro-ring modulator," in IEEE Photonics Technology Letters, vol. 32, no. 2, pp. 125-128, 15 Jan.15, 2020, doi: 10.1109/LPT.2019.2960238.

[6] C. Minkenberg et al., "Reimagining datacenter topologies with integrated silicon photonics," J. Opt. Commun. Netw., vol. 10, no. 7, p. B126, 2018

[7] P. Srinivasan et al., "Hybrid O-band electro-absorption modulators on multi-micron waveguide silicon photonics platform for optical engine applications," 45th European Conference on Optical Communication (ECOC 2019), 2019, pp. 1-3, doi: 10.1049/cp.2019.0853.

[8] J. Lambrecht et al., "Low-Power (1.5 pJ/b) silicon integrated 106 Gb/s PAM-4 optical transmitter," in Journal of Lightwave Technology, vol. 38, no. 2, pp. 432-438, 15 Jan.15, 2020, doi: 10.1109/JLT.2019.2933286.

[9] A. H. Talkhooncheh, A. Zilkie, G. Yu, R. Shafiiha and A. Emami, "A 100 Gb/s PAM-4 Silicon Photonic Transmitter with Two Binary-Driven EAMs in MZI Structure," 2021 IEEE Photonics Conference (IPC), 2021, pp. 1-2, doi: 10.1109/IPC48725.2021.9593028.